THE JOURNAL OF PHYSICAL CHEMISTRY B
A JOURNAL OF THE AMERICAN CHEMICAL SOCIETY

pubs.acs.org/JPCB

Article

Synergism in the Molecular Crowding of Ligand-Induced Riboswitch Folding: Kinetic/Thermodynamic Insights from Single-Molecule Spectroscopy

Hsuan-Lei Sung and David J. Nesbitt*

Cite This: *J. Phys. Chem. B* 2022, 126, 6419−6427

Read Online

ACCESS | Metrics & More | Article Recommendations

ABSTRACT: Conformational dynamics in riboswitches involves ligand binding and folding of RNA, each of which can be influenced by excluded volume effects under "crowded" *in vivo* cellular conditions and thus incompletely characterized by *in vitro* studies under dilute buffer conditions. In this work, temperature-dependent single-molecule fluorescence resonance energy transfer (FRET) spectroscopy is used to characterize the thermodynamics of (i) cognate ligand and (ii) molecular crowders (PEG, polyethylene glycol) on folding of the *B. subtilis LysC* lysine riboswitch. With the help of detailed kinetic analysis, we isolate and study the effects of PEG on lysine binding and riboswitch folding steps individually, from which we find that PEG crowding facilitates riboswitch folding primarily via a surprising *increase in affinity for the cognate ligand*. This is furthermore confirmed by temperature-dependent studies, which reveal that PEG crowding is not purely entropic and instead significantly impacts both enthalpic and entropic contributions to the free energy landscape for folding. The results indicate that PEG molecular crowding/stabilization of the lysine riboswitch is more mechanistically complex and requires extension beyond the conventional picture of purely repulsive solvent−solute steric interactions arising from excluded volume and entropy. Instead, the current experimental FRET data support an alternative multistep mechanism, whereby PEG first entropically crowds the unfolded riboswitch into a "pre-folded" conformation, which in turn greatly increases the ligand binding affinity and thereby enhances the overall equilibrium for riboswitch folding.

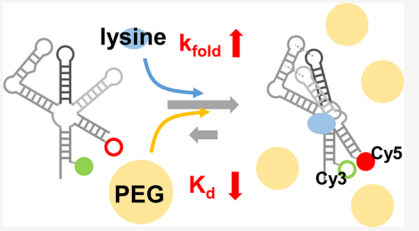

1. INTRODUCTION

Intracellular environments are highly concentrated with various kinds of solutes ranging from small molecule metabolites to macromolecule proteins and nucleic acids.[1] All these solutes impose ubiquitous steric constraints (such as excluded volume) that affect both biomolecular structure and function.[2,3] Simply summarized, the presence of solute limits the space available for the biomolecule to sample and thereby entropically favors any conformations that occupy smaller volume.[4] Such steric stabilization toward more compact biomolecule structures is often referred to as molecular crowding.[5,6]

Most biochemical studies are performed in dilute buffer, which differs significantly from the in vivo intracellular environment where biomolecules actually function. In order to correctly interpret these in vitro observations, therefore, it is crucial to characterize and understand the effects of crowding on biomolecular systems.[7−9] Experimentally, polymeric crowders such as PEG (polyethylene glycol) and dextran (polysaccharide) are often introduced into biological buffers to mimic the intracellular crowding environment.[10] Consistent with simple crowding expectations, the presence of such polymers favors the more compact biomolecular conformation.[11] Interestingly, many of these studies identified the origin of such polymer stabilization[12−14] to be largely entropic in nature, suggesting that the interaction between polymer crowders and a crowded biomolecule occurs predominantly via the effective "repulsion" because of pure excluded volume effects.[15]

Riboswitches are RNA elements that regulate gene expression in response to ligand concentrations in the cell.[16,17] In particular, folding of the lysine riboswitch is found to be facilitated by ligands through an induced-fit (IF, "bind-then-fold") mechanism,[18,19] whereby the presence of lysine binding lowers the free energy activation barrier and thereby promotes subsequent folding of the riboswitch. As indicated in Figure 1A, the binding of lysine (with dissociation constant K_d) is a prerequisite for riboswitch folding; the lysine-associated riboswitch can then fold and unfold at the rate of k_{fold} and k_{unfold}, respectively. Because molecular crowding effects can in principle impact both binding and folding

Received: May 20, 2022
Revised: August 2, 2022
Published: August 18, 2022

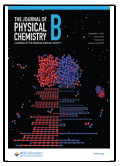

https://doi.org/10.1021/acs.jpcb.2c03507
J. Phys. Chem. B 2022, 126, 6419−6427

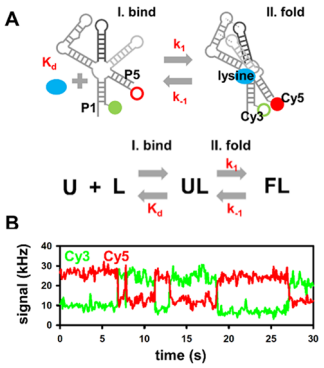

Figure 1. Schematic presentation of lysine riboswitch single-molecule FRET construct folding. (A) Induced-fit mechanism of lysine riboswitch folding where I. lysine binding is followed by II. the riboswitch conformational change (U = unfolded riboswitch, F = folded riboswitch, and L = lysine). Note that folding brings Cy3 and Cy5 closer and thereby increases the FRET energy transfer efficiency (E_{FRET}). (B) Sample time-dependent fluorescent signal. The conformational change is visualized by the anticorrelation between the Cy3 and Cy5 signal, which results in E_{FRET} changes.

steps,[20−24] this necessitates further study into kinetic and thermodynamic mechanisms for crowding and ligand-induced riboswitch folding, in order to deconstruct their respective influences on riboswitch function and resulting gene expression.

In this work, we explore the effects of PEG on the lysine riboswitch folding with single-molecule fluorescence resonance energy transfer (FRET) spectroscopy. In the context of simple nucleic acid constructs, PEG has been found to facilitate secondary and tertiary folding via predominantly entropic effects,[25] such as would be consistent with a "hard sphere" physical picture of crowding. Specifically, previous PEG crowding studies as a function of temperature highlight the negligible role of differential enthalpic effects in RNA/DNA conformational change. From the detailed kinetic analysis of the single-molecule data, however, one can characterize the overall riboswitch folding by two sequential mechanistic pathways: (i) ligand binding and (ii) subsequent conformational change of the lysine riboswitch,[26] thereby motivating study of the impact of PEG crowding on each of these processes separately. Moreover, single-molecule experiments as a function of temperature enable further deconstruction of free energies and free energy barriers into enthalpic and entropic contributions along the folding coordinate.[27] As a result, the work potentially provides new thermodynamic and kinetic insights into the effect of molecular crowding on both RNA-small molecule binding and evolution of the lysine riboswitch from unfolded to "pre-folded" to folded conformations.

2. EXPERIMENT

2.1. Lysine Riboswitch Construct and Sample Preparation. In this work, we use a modified *B. subtilis lysC* lysine riboswitch[28] as a model system to explore the effect of crowding on ligand-induced RNA folding. The doubly dye-labeled and biotinylated RNA construct is synthesized by annealing three strands of nucleic acid oligomers together (Figure 1A, the biotinylated P1 extension not shown).[18] The distal ends of stem P1 and P5 are labeled with the cyanine dyes Cy3 and Cy5, respectively, to maximize the E_{FRET} (FRET energy transfer efficiency) contrast during the conformational change in response to lysine.[29] Details of the RNA sequences and synthesis methods can be found in previous work.[18] We note that conformational changes for the model construct are consistent with the wild-type riboswitch, as the E_{FRET} values observed can be reliably predicted from the crystal structure.[28] The ligand affinity of the model construct under physiological Mg^{+2} conditions ($K_D \approx 0.7$ mM) is lower than that of the wild-type riboswitch at higher Mg^{+2} ($K_D \approx 1$ μM).[30] Such differential sensitivity arises from the significantly higher Mg^{2+} concentrations (20 mM) used in previous structural analyses (e.g., in-line probing) of the wild-type RNA.[30]

To prepare samples for single-molecule experiments, the coverslip sample holder is first incubated with 10% biotinylated BSA (bovine serum albumin) to prevent nonspecific binding. A

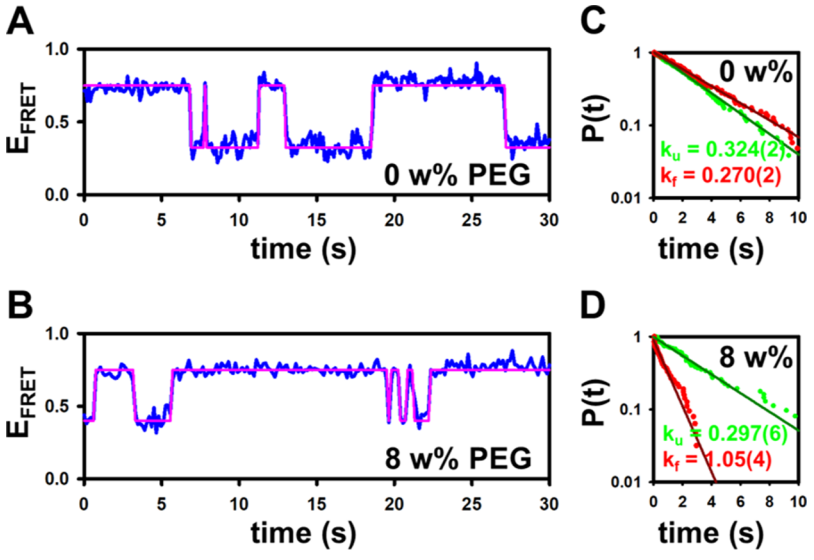

Figure 2. Sample E_{FRET} trajectories and dwell time analysis. (A) E_{FRET} trajectories without PEG. (B) E_{FRET} trajectories with 8 wt % PEG. Note that the construct spends significantly more time in the high E_{FRET} state corresponding to the folded conformation. (C) Dwell time analysis without PEG. (D) Dwell time analysis with 8 wt % PEG. The cumulative distribution function of the unfolded dwell time decays much more rapidly, corresponding to accelerated k_{fold}.

https://doi.org/10.1021/acs.jpcb.2c03507
J. Phys. Chem. B 2022, 126, 6419−6427

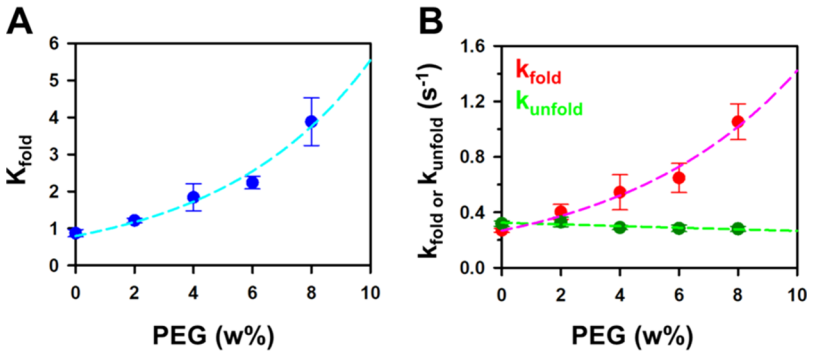

Figure 3. PEG-dependent lysine riboswitch folding at a constant lysine concentration (1 mM). (A) Folding equilibrium and (B) kinetics as a function of PEG concentration. Data are fit to a single exponential function to highlight the rapid rise of K_{fold} and k_{fold} with increasing PEG concentration.

second incubation step results in sufficient streptavidin attachment to the coverslip, with surface tethering of the riboswitch construct achieved by biotin−streptavidin association. Single-molecule fluorescence experiments are performed under buffer conditions with (i) 50 mM HEPES (pH 7.5), 100 mM NaCl, 50 mM KCl, and 0.5 mM $MgCl_2$ to provide sufficient background cations and maintain the buffer pH, (ii) Trolox/PCA/PCD oxygen scavenger system to enhance fluorophore photostability,[31] and (iii) additional lysine and PEG 3k (average molecular weight ≈3000 amu) to achieve the desired experimental crowding conditions.

2.2. Temperature-Controlled Single-Molecule Experiment and Data Analysis. The present single-molecule FRET experiments have been performed with a through-objective total internal reflection fluorescence (TIRF) microscope, with details described elsewhere.[32] In brief, a 532 nm laser beam is directed through a high numerical aperture oil-immersion microscope objective, with a mirror set for parallel translation of the beam with respect to the objective axis to increase the incident angle and thereby achieve total internal reflection illumination of fluorescent RNA constructs immobilized at the coverslip−water interface. The resulting fluorescence from the sample is then collected by the same wide-field objective, split by a dichroic mirror into Cy3 and Cy5 channels, and focused onto a charge-coupled device (CCD) video camera, with which data are collected in a video format at a 20 Hz acquisition frame rate (Figure 1B).

Single-molecule fluorescent traces are obtained from the recorded movie by custom analysis software with background correction to generate the resulting E_{FRET} time trajectory (see sample data in Figure 2A, B). A standard hidden Markov modeling method is used to identify transitions between the folded (E_{FRET} ∼ 0.7) and the unfolded (E_{FRET} ∼ 0.3 to 0.4) conformations and thereby to acquire individual dwell times.[33] The folding equilibrium constant K_{fold} can be readily extracted as the ratio of total folding and unfolding dwell times ($K_{fold} = T_{fold}/T_{unfold}$), from which the folded fraction F_{fold} can be calculated ($F_{fold} = T_{fold}/(T_{fold} + T_{unfold})$). The folding ($k_{fold}$) and unfolding ($k_{unfold}$) rate constants themselves can be obtained from the analysis of the corresponding dwell time distributions for t_{unfold} and t_{fold} (see sample data in Figure 2C, D), respectively.[34] Cumulative distributions for both t_{fold} and t_{unfold} are well fit to single exponential decay functions, consistent with folding and unfolding of the lysine riboswitch well described by simple first order kinetics. Note that each cumulative distribution function ($N = 3$) consists of dwell times obtained from ≈10 individual molecules within 1 or 2 surface scans. The uncertainties (e.g., error bars in Figures 3−7) are reported as the standard deviation of the mean. We believe that the major source of measurement uncertainties is the sample heterogeneity, along with minor contributions from fitting errors and temperature fluctuation.

The temperature-controlled single-molecule studies are achieved with the help of thermoelectric cooling/heating modules under servo loop control, as described in previous work.[32] Both the sample and microscope objectives are cooled/heated simultaneously to minimize any thermal gradients across the sample, with sample temperatures measured (to ±0.1 °C accuracy) using a calibrated resistance thermometer.

3. RESULTS AND ANALYSIS

3.1. Lysine Riboswitch Folding Promoted by PEG. Previous studies have shown that folding kinetics of the lysine riboswitch follows an induced-fit (IF) mechanism,[18,19] whereby lysine binding is an essential prerequisite for the riboswitch to fold. Under 1.0 mM lysine conditions, the riboswitch spends roughly equal average amounts of time in the high E_{FRET} (E_{FRET} ∼ 0.7) and low E_{FRET} (E_{FRET} ∼ 0.3) states, corresponding to the folded and unfolded conformations (Figure 2A). Additional 8 wt % (percentage by weight) of PEG significantly promotes equilibrium folding of the riboswitch, as evident in the greatly enhanced time durations the fluorescent construct spends in the high E_{FRET} state (Figure 2B). Furthermore, at constant 1 millimolar lysine concentration, K_{fold} increases monotonically (Figure 3A) with systematically increasing PEG, again consistent with crowding promotion of the folded riboswitch conformation under equilibrium conditions.

In addition to the above equilibrium data, however, an even greater wealth of information on single-molecule biophysical kinetics is revealed in dwell time distributions for each fluorescence trajectory. In particular, kinetic information in these single-molecule fluorescence trajectories can be obtained from logarithmic dwell time analysis of the cumulative probability distributions,[34] with sample data under low (0 wt % PEG) and high (8 wt % PEG) crowding conditions displayed in Figure 2C, D. These data make clear that PEG dramatically increases the folding rate (k_{fold}, in red) and decreases the unfolding rate (k_{unfold}, in green) of the lysine riboswitch (Figure 3B). In particular, the crowding effects are much stronger on the folding vs unfolding step. Specifically,

https://doi.org/10.1021/acs.jpcb.2c03507
J. Phys. Chem. B 2022, 126, 6419−6427

there is a nearly 400% increase in k_{fold} between 0 and 8 wt % PEG concentrations, over which range k_{unfold} is reduced by only 10%.

3.2. PEG Stabilization on Lysine-Dependent Folding Illustrated by Kinetic Modeling. Here, we implement a more detailed kinetic analysis to highlight the PEG effect on the ligand response of the riboswitch folding.[26] In previous work, folding of the lysine riboswitch was found to be initiated by ligand association, followed by RNA conformational change in a "bind-then-fold" induced-fit (IF) mechanism.[18,19] The simplified IF folding pathway is illustrated in Figure 1A, where K_d reflects the dissociation constant of lysine and k_1/k_{-1} corresponds to unimolecular forward/backward rate constants for overall conformational changes in the riboswitch construct.

We first focus on the equilibrium folding behavior by studying the folded fraction $F_{fold} = T_{fold}/(T_{fold} + T_{unfold})$ as a function of lysine at a constant PEG concentration (Figure 4).

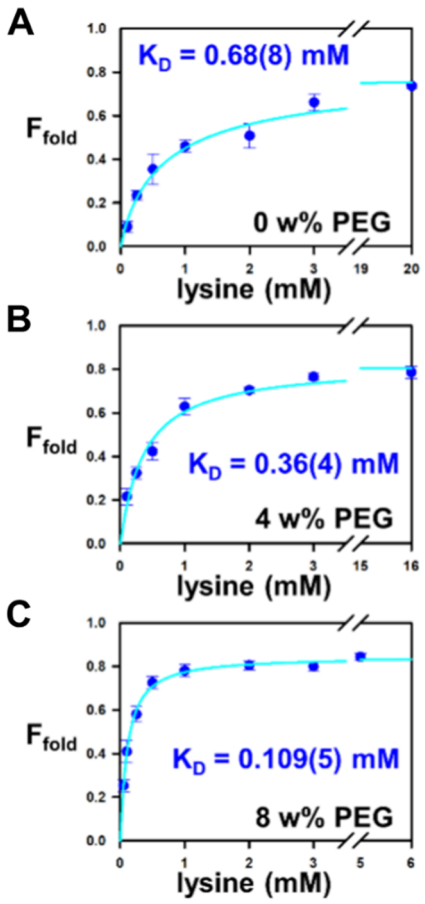

Figure 4. Lysine-dependent folding curves at a series of PEG concentrations. Folded fraction F_{fold} as a function of lysine with (A) 0 wt %, (B) 4 wt %, and(C) 8 wt % PEG. Data are nonlinear least squares fit to the Hill equation (eq 1).

As expected, the data indicate linear growth in F_{fold} at low ligand concentrations and eventual saturation at high lysine. More surprising is the dependence of these curves on crowder, with the saturation plateau quite insensitive to PEG from 0 to 8 wt %, yet with the lysine binding affinity increasing by nearly an order of magnitude over the same range of crowding conditions. Simply summarized, the main role of PEG as a molecular crowder appears to be through the promotion of the lysine riboswitch binding interaction, which in turn facilitates subsequent folding of the riboswitch. It is worth noting that the enhancement of bimolecular association is expected from PEG crowding. To highlight more quantitatively the impact of PEG on lysine-induced riboswitch folding, the data can be fit to the Hill equation:[35]

$$F_{fold} = F_{max} \times \frac{[lysine]^{n_1}}{K_D^{n_1} + [lysine]^{n_1}} \quad (1)$$

where n_1 is the Hill coefficient, K_D is the effective dissociation constant for lysine binding, and F_{max} corresponds to the maximal F_{fold} value under saturated lysine conditions. Because K_D corresponds to the lysine concentration for which $F_{fold} = F_{max}/2$, a smaller K_D value reflects a more effective lysine promotion of riboswitch folding. The fitting results are summarized in Table 1 for 0 to 8 wt % PEG crowder

Table 1. Least Squares Fit Results for the Lysine-Induced Folding Equilibria

	K_D (mM)	n_1	F_{max}
0 wt % PEG	0.68(8)	0.91(9)	0.77(2)
4 wt % PEG	0.36(4)	1.02(12)	0.82(2)
8 wt % PEG	0.109(5)	1.08(6)	0.843(10)

conditions, over which K_D reduces from 0.68(8) to 0.109(5) mM, corresponding to an equivalent 7-fold efficiency increase in lysine-promoted riboswitch folding with a $n_1 \approx 1$ (i.e., noncooperative) Hill coefficient.

The kinetic promotion of lysine-induced riboswitch folding can also be investigated via statistical analysis of the dwell time distributions (see Figure 5), for which the effective folding rate constant (k_{fold}) increases as a function of lysine and eventually reaches a saturation plateau. By way of contrast, the unfolding rate constant k_{unfold} is completely insensitive to lysine and remains constant over a wide range of ligand concentrations.[18] Such kinetic results are in fact entirely consistent with an induced-fit mechanism, whereby lysine promotes riboswitch folding through a "bind-then-fold" process.[18,19] Specifically for such a simplified kinetic model (see Figure 1A), increase in lysine concentration simply shifts the equilibrium toward a higher fraction in the ligand bound state, thereby promoting the effective unimolecular folding rate k_{fold} up to the limiting velocity of k_1. Conversely, the effective unimolecular unfolding rate k_{unfold} simply reflects k_{-1} and remains independent of lysine concentration.[26] By solving the kinetic equations assuming rapid equilibration with respect to lysine binding, the data can be fit to an independent Hill equation for k_{fold}:[26]

$$k_{fold} = k_1 \times \frac{[lysine]^{n_2}}{K_d^{n_2} + [lysine]^{n_2}} \quad (2)$$

where again n_2 is a Hill coefficient, K_d is the lysine dissociation constant, and k_1 corresponds to the maximal k_{fold} value under saturating ligand conditions. Similar to the results discussed above for folding/unfolding equilibrium constant properties, we find that the addition of the PEG crowder significantly increases the efficiency for lysine binding (i.e., reduces K_d) and in turn facilitates folding of the lysine riboswitch. Interestingly, by the way of comparison, only relatively modest PEG effects on the elemental folding/unfolding rate processes are observed, with 8 wt % PEG concentrations increasing/decreasing the unimolecular folding (k_1)/unfolding (k_{-1}) rate constants by only 10%/40%, respectively. Such relatively

https://doi.org/10.1021/acs.jpcb.2c03507
J. Phys. Chem. B 2022, 126, 6419−6427

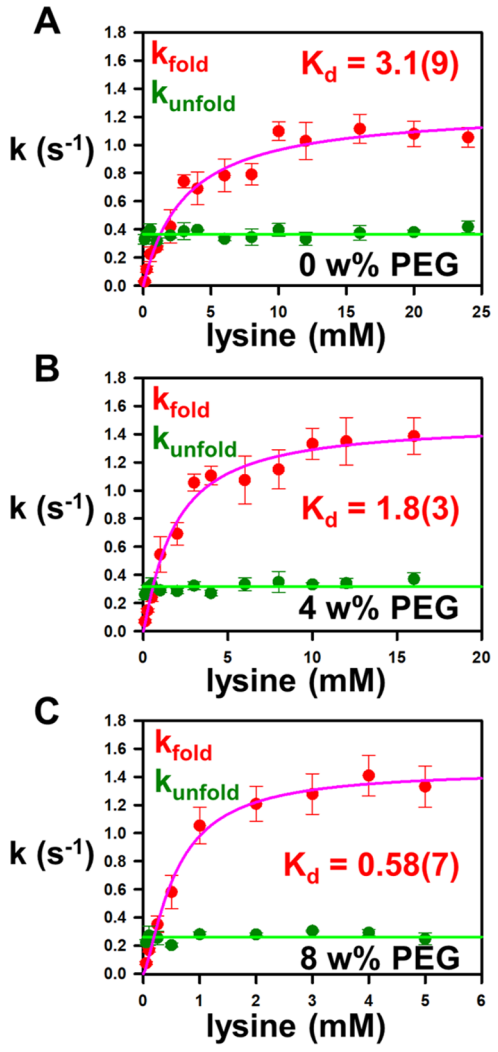

Figure 5. Lysine-dependent folding and unfolding rates at a series of PEG concentrations. Folding rate constants k_{fold}/k_{unfold} as a function of lysine with (A) 0 wt %, (B) 4 wt %, and (C) 8 wt % PEG. The k_{fold} data are fit to the Hill-like kinetic equation (eq 2), while the lysine-independent k_{unfold} data are fit with a horizontal line.

modest changes in the intrinsic rates are consistent with crowding,[14] with fits of the kinetic data to eq 2 summarized in Table 2. However, it is worth stressing that the predominant impact of molecular crowding from this mechanistic perspective arises from a 7× decrease in K_d (i.e., 700% enhancement of ligand binding to the riboswitch).

Table 2. Least Squares Fit Results for the Lysine-Induced Folding Kinetics

	K_d (mM)	n_2	k_1 (s^{-1})	k_{-1} (s^{-1})
0 wt % PEG	3.1(9)	1.00(19)	1.26(13)	0.367(8)
4 wt % PEG	1.8(3)	1.12(17)	1.48(10)	0.317(9)
8 wt % PEG	0.58(7)	1.34(17)	1.45(6)	0.262(11)

3.3. Temperature-Dependent Folding Reveals Both Enthalpic and Entropic PEG Effects. We can take such equilibrium and kinetic analyses one important step further by performing temperature-dependent smFRET folding experiments, which permit deconstruction of overall (ΔG^0) and transition state ($\Delta G^{\ddagger}$) free energies into enthalpic (ΔH) and entropic (ΔS) contributions as a function of PEG crowder concentrations. First of all, studies in the absence of a crowder reveal that unfolding of the lysine riboswitch is strongly favored with increasing temperature, specifically 10-fold reduction in the overall equilibrium constant K_{fold} over a modest 12 °C temperature range. Quantitative thermodynamic information for the corresponding folding enthalpy and entropies can be extracted from a simple van't Hoff analysis, that is,

$$\ln K_{fold} = -\frac{\Delta H^0}{R}\frac{1}{T} + \frac{\Delta S^0}{R} \quad (3)$$

As summarized in the sample data in Figure 6A, B, overall folding of the lysine riboswitch at both low (0 wt %) and high (6 wt %) crowder conditions is found to be exothermic (ΔH^0 = −32.8(18) and −15.0(14) kcal/mol, respectively) and yet entropically penalized ($-T\Delta S^0$ = −111(5) and −50(3) cal/mol/K), consistent with a simple physical picture of folding, whereby biomolecules are enthalpically encouraged to fold into a more ordered (lower entropy) state.[36] Of particular interest, however, the addition of 6 wt % PEG (Figure 6B) decreases and increases the slopes vs intercepts, corresponding to incremental PEG-induced increase in both ΔH^0 and ΔS^0 ($\Delta\Delta H^0 > 0$ and $\Delta\Delta S^0 > 0$). Simply stated, the presence of the PEG crowder reduces the thermodynamic advantage of folding exothermicity and yet also lowers the entropic penalty for folding of the lysine riboswitch. We will return to this important issue in the Discussion section, but for the moment, we emphasize that such changes in the overall exothermicity

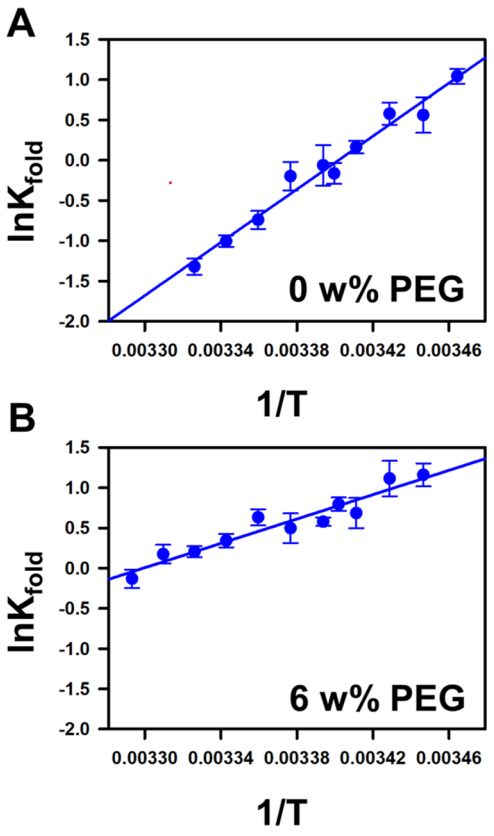

Figure 6. van't Hoff plots for the temperature-dependent lysine riboswitch folding at (A) 0 wt % PEG and (B) 6 wt % PEG. [lysine] = 1 mM.

https://doi.org/10.1021/acs.jpcb.2c03507
J. Phys. Chem. B 2022, 126, 6419−6427

($\Delta\Delta H^0 > 0$) with PEG concentration *are inconsistent with a purely excluded volume interpretation of crowding*, for which the driving forces are predicted to be purely entropic ($\Delta\Delta S^0 > 0$).

There is of course additional thermodynamic information in the temperature dependence of the kinetic rate constants themselves. Specifically, if we make the plausible assumption of a single rate-limiting transition state, we can similarly analyze the temperature-dependent kinetic data with the transition state/Eyring theory.[37−39]

$$\ln k = -\frac{\Delta H^{\ddagger}}{R}\frac{1}{T} + \frac{\Delta S^{\ddagger}}{R} + \ln \nu \tag{4}$$

where $\Delta H^{\ddagger}$ and $\Delta S^{\ddagger}$ represent enthalpic and entropic differences, respectively, between the transition state and the folded/unfolded states of the riboswitch. In eq 4, ν represents the attempt frequency (set to be 10^{13} s^{-1} in our analysis) to access the transition barrier along the folding/unfolding coordinate,[40] although the extracted value of $\Delta S^{\ddagger}$ is only logarithmically dependent on such a choice. Despite the fact that any absolute entropy change associated with surmounting the transition state barrier will depend weakly on the choice of ν, any differential changes in entropy ($\Delta\Delta S^{\ddagger}$) induced by PEG crowding remain rigorously independent of any such logarithmic offset.

As clearly evident in Figure 7A, the logarithmic rate constant from such an Arrhenius analysis for folding of the lysine riboswitch increases linearly with $1/T$. The slope in Figure 7A (red line) implies that folding of the riboswitch releases heat ($\Delta H_{fold}^{\ddagger} \approx -17.3(16)$ kcal/mol) in accessing the transition state, while the negative intercept ($\Delta S_{fold}^{\ddagger} \approx -121(3)$ cal/mol/K) indicates an entropic TS barrier ($-T\Delta S_{fold}^{\ddagger} > 0$) in the absence of crowding conditions. In the presence of 6 wt % PEG crowder (see Figure 7B), the slope and intercept of the Eyring plot change rather dramatically for k_{fold}, corresponding to a significant differential decrease in both exothermicity ($\Delta\Delta H_{fold}^{\ddagger} > 0$) and entropic cost ($-T\Delta\Delta S_{fold}^{\ddagger} < 0$) for access to the folding transition state. Of particular interest and in contrast with the riboswitch folding kinetics, however, the presence of 6 wt % PEG molecular crowders results in very modest effects on the temperature dependence of k_{unfold}, with therefore only small crowding-induced changes in enthalpy ($\Delta\Delta H_{unfold}^{\ddagger} \approx 0$) and entropy ($(-T\Delta\Delta S_{unfold}^{\ddagger} \approx 0$) required to reach the transition state from the fully folded lysine riboswitch conformation.

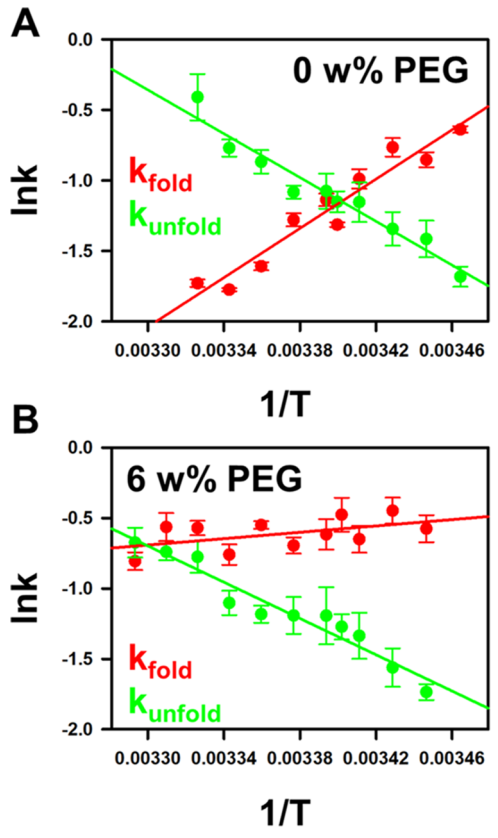

Figure 7. Eyring plots for the temperature-dependent lysine riboswitch folding at (A) 0 wt % PEG and (B) 6 wt % PEG. [lysine] = 1 mM.

4. DISCUSSION

4.1. Kinetic vs Thermodynamic Crowding Data Indicate Conflicting Solute Interaction Models. We have shown that the lysine riboswitch folding can be promoted by increasing PEG concentration, which is entirely consistent with crowding effects, where the presence of PEG favors the more compact state.[13,14] From the perspective of the solute interaction model, such PEG-enhanced structure formation can simply result from generic repulsion between PEG and the RNA.[41] Specifically, the biomolecule might tend to adopt the more compact conformation in order to reduce the solvent-accessible surface area (SASA) and in turn decrease overall unfavorable solute−biomolecule contact.[42,43] Taking these ideas one step further, if this repulsion was shown to be predominantly steric (i.e., entropic) in nature, it can be unambiguously attributed to the crowding effects originating from the excluded volume.[13] However, the significant slope changes in the van' Hoff plots in Figure 6 signal differential enthalpic contributions and may suggest a more complex solute effect, which we can explore further.

The thermodynamic parameters obtained from temperature dependence are summarized in Figure 8, where the relative enthalpy and entropy of each state are plotted along the simplified folding coordinate, with the folded state F referenced to zero.[35] It is shown that PEG exerts effects (red vs blue) predominantly on the (forward) folding activation enthalpy ($\Delta H_{fold}^{\ddagger}$) and entropy ($\Delta S_{fold}^{\ddagger}$), while leaving the relative free energy contributions between the transition state and the folded state largely unperturbed (Figure 8B, C). Furthermore, the shifts in Figure 8 suggest the unfolded conformation is enthalpically stabilized and entropically destabilized by PEG with respect to the transition/folded states. From the physical picture of a simple solute interaction model, such a free energy change corresponds to an increase in PEG association with the unfolded conformation of larger SASA.[25] In other words, our thermodynamic analysis reveals an overall attraction (favorable contact) between PEG and the riboswitch.

Indeed, solvent−solute interactions represent a simple yet efficient way to understand solute-promoted biomolecule folding/unfolding. However, the thermodynamic results for preferential PEG solvation of the unfolded state clearly contradict the general repulsion between PEG and RNA predicted from the PEG-enhanced lysine riboswitch folding. It is in fact unusual for favorable PEG−RNA contacts to enhance folding, which requires increasing the area of the RNA−RNA interface. Such discrepancies suggest that solute interactions

https://doi.org/10.1021/acs.jpcb.2c03507
J. Phys. Chem. B 2022, 126, 6419−6427

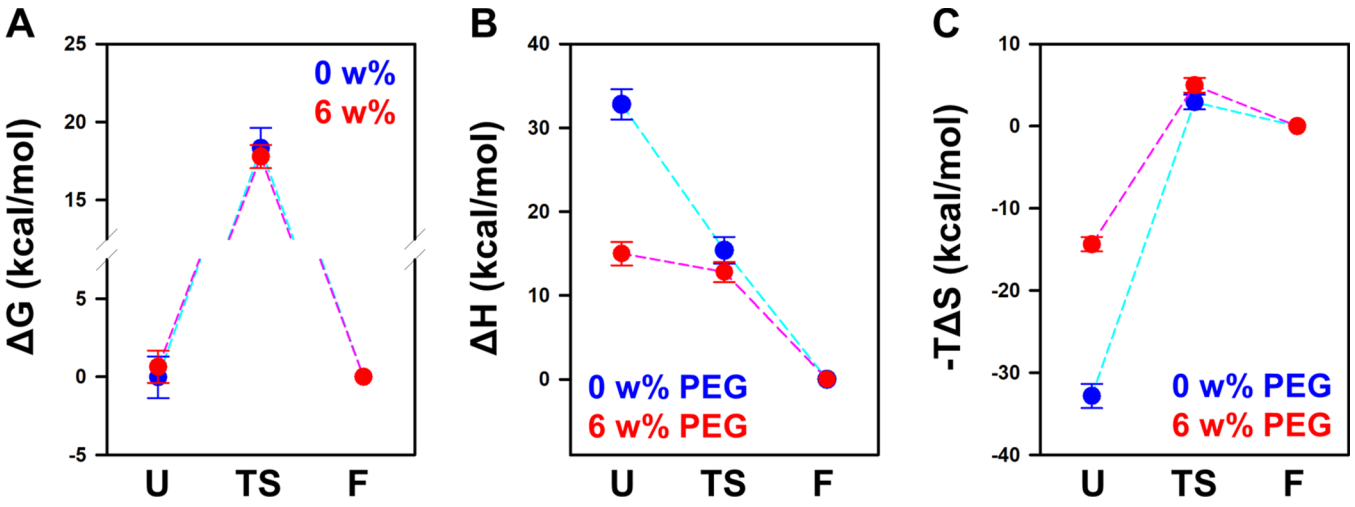

Figure 8. Free energy landscapes for lysine riboswitch folding. PEG effects on the (A) free energy, (B) enthalpic, and (C) entropic contributions along the folding coordinate (U = unfolded state, TS = transition state, and F = folded state). Values are arbitrarily referenced to zero for the folded state F.

alone are insufficient to account for our present findings, with a much more likely hybrid folding mechanism required for the observed changes in both entropy and enthalpy with crowding conditions.

4.2. PEG Prearranges the Unfolded Riboswitch To Facilitate Folding. Careful inspection of the E_{FRET} trajectories in Figure 2 show the low E_{FRET} state of the lysine riboswitch shifts to a slightly higher value (from ≈0.3 to 0.4, as illustrated in Figure 9) by PEG when the riboswitch becomes

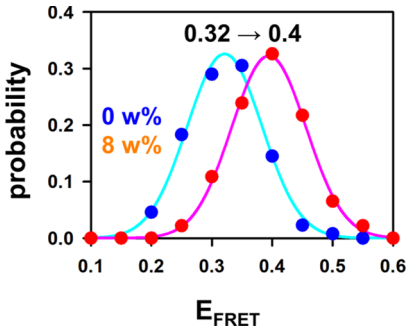

Figure 9. Normalized E_{FRET} distribution of the low E_{FRET} population with 0 wt % PEG (blue) and 8 wt % PEG (red). Bin size = 0.05.

more folded. Such an observation indicates that PEG may not only promote the overall riboswitch folding but also alter the structure of the unfolded (relatively low E_{FRET}) state. A similar behavior is also observed in previous single-molecule studies of the lysine riboswitch,[18,29,44] where the low E_{FRET} value increases in response to buffer conditions that promote folding. Moreover, one study is able to resolve the low E_{FRET} population of the same *lysC* riboswitch into (i) the fully unfolded and (ii) the lysine-free pre-folded states.[44] We, therefore, suspect that equilibrium between the unresolved low E_{FRET} conformations may have significant impact on our thermodynamic analysis.

Although we are unable to resolve, assign, and deconvolute these low E_{FRET} conformations in the kinetics, we can treat the low E_{FRET} state as an average of (1) the fully unfolded and (2) the pre-folded conformations, as the simplest physical model to understand the thermodynamic consequence. The slightly elevated E_{FRET} value indicates that PEG drives the equilibrium from the unfolded to a "pre-folded" lysine riboswitch, which is consistent with the common observation of PEG promoting the formation of the structure. Because the low E_{FRET} state is already partially folded by PEG, we therefore expect a lower enthalpic gain accompanied by a lower entropic penalty for folding, with these predictions clearly confirmed in Figure 8. Moreover, the previous study has demonstrated that this pre-folded state has stronger lysine affinity and thus higher tendency to fold,[44] which agrees completely with the rapidly decreasing lysine dissociation constants (K_D and K_d) by PEG observed in our detailed kinetic analysis (Figure 4). It is worth noting that a similar mechanism of solute facilitating folding by "pre-organization" of the unfolded state has also been observed in several riboswitch systems.[26,34,45]

The addition of a postulated pre-folded state provides a more reasonable and plausible mechanism, with which the present kinetic and thermodynamic data can be explained. Because the thermodynamics of lysine riboswitch folding is dominated by rapid equilibrium between the two low E_{FRET} (unfolded/prefolded) conformations, we lose the information on the PEG−RNA interaction except for the fact that PEG increases the overall riboswitch (pre-)folding. It has been previously shown that the interactions between PEG and nucleic acid secondary/tertiary structures are predominantly entropic and therefore consistent with crowding via fundamental excluded volume interactions.[25] In fact, it was surprising in this study to see any PEG-dependent differential enthalpy effects for lysine riboswitch folding, as we do not expect significant changes in thermodynamic properties between simple nucleic acid folding motifs to the more complex structure of a riboswitch.[46,47] With the partially folded state included as part of the low E_{FRET} population, we cannot rule out excluded volume effects as the predominant reason behind any PEG-dependent changes in riboswitch conformation, despite significant enthalpic contributions to the overall thermodynamics. In fact, the observation that the lysine-saturated folding (k_1)/unfolding (k_{-1}) rate constants increase/decrease, respectively, as a function of the PEG concentration is entirely consistent with simple crowding predictions.[14] This prompted our suggestion of an alternative albeit simple three-

https://doi.org/10.1021/acs.jpcb.2c03507
J. Phys. Chem. B 2022, 126, 6419−6427

state (unfolded ⇌ "prefolded" ⇌ folded) kinetic mechanism, whereby crowding is able to manifest itself via both enthalpic and entropic changes in the thermodynamics, in addition to recapitulating the physically correct kinetic and thermodynamic basis for PEG-promoted lysine riboswitch folding.

5. SUMMARY AND CONCLUSIONS

We use the single-molecule FRET methods to characterize the ligand-induced RNA folding motif in response to common crowding agent PEG, for which PEG promotes the overall RNA folding by increasing k_{fold} and decreasing k_{unfold} simultaneously. With detailed kinetic analysis, we find the most prominent PEG effect is to facilitate the lysine binding and thereby promote the overall structural change of the riboswitch. Such kinetic effects are consistent with a simple physical picture of repulsive interactions between PEG and the surface of the riboswitch and/or lysine. However, the reduced exothermicity and entropic penalty for folding observed in the temperature-dependent studies suggests that PEG preferentially solvates the unfolded state because of its larger surface area.[48] Such a discrepancy suggests the PEG effects cannot be simply understood by the very common physical picture of purely "repulsive" solute−biomolecule interactions. Further motivated by additional structural information from small E_{FRET} shifts, we therefore propose a simple physical model with an additional "pre-folded" low E_{FRET} state that nicely accounts for both the thermodynamic and kinetic findings. In the model, PEG prearranges the unfolded conformation of the riboswitch and shifts the E_{FRET} to slightly higher values, as evidenced in our single-molecule E_{FRET} trajectories. From our kinetic analysis, we find the more fold-like, but the ligand-free riboswitch has a much higher tendency to bind a lysine molecule and proceed to fold. On the other hand, the partially formed riboswitch structure also reduces the folding exothermicities and entropic penalties, as seen in the temperature-dependent studies. Furthermore, the proposed three-state model provides an alternative mechanism for purely entropic crowding to induce secondary changes in the overall RNA folding enthalpy that are consistent with experimental observation. Although this will require confirmation by additional single-molecule temperature-dependent studies, the net effect is an extension of simple excluded volume models that can correctly predict both entropic and enthalpic contributions to the crowding process occurring in the cellular environment.

AUTHOR INFORMATION

Corresponding Author

David J. Nesbitt − *JILA, National Institute of Standards and Technology and University of Colorado, Boulder, Colorado 80309, United States; Department of Chemistry and Department of Physics, University of Colorado, Boulder, Colorado 80309, United States;* orcid.org/0000-0001-5365-1120; Email: djn@jila.colorado.edu

Author

Hsuan-Lei Sung − *JILA, National Institute of Standards and Technology and University of Colorado, Boulder, Colorado 80309, United States; Department of Chemistry, University of Colorado, Boulder, Colorado 80309, United States*

Complete contact information is available at: https://pubs.acs.org/10.1021/acs.jpcb.2c03507

Notes

The authors declare no competing financial interest.

ACKNOWLEDGMENTS

Initial support for this work has been through the National Science Foundation under grants CHE 1665271/2053117 from the Chemical, Structure, Dynamics and Mechanisms-A Program, with recent transition support from the Air Force Office of Scientific Research (FA9550-15-1-0090) and additional funds for the development of the confocal apparatus from PHY-1734006 (Physics Frontier Center Program). We would also like to acknowledge early seed contributions by the W. M. Keck Foundation Initiative in RNA Sciences at the University of Colorado, Boulder, as well as thank David Nicholson and Andrea Marton Menendez for assistance with the TIRF microscope.

REFERENCES

(1) Fulton, A. B. How Crowded is the Cytoplasm? *Cell* **1982**, *30*, 345−347.

(2) Minton, A. P. Excluded Volume as a Determinant of Macromolecular Structure and Reactivity. *Biopolymers* **1981**, *20*, 2093−2120.

(3) Ellis, R. J. Macromolecular Crowding: Obvious but Underappreciated. *Trends Biochem. Sci.* **2001**, *26*, 597−604.

(4) Minton, A. P. The Influence of Macromolecular Crowding and Macromolecular Confinement on Biochemical Reactions in Physiological Media. *J. Biol. Chem.* **2001**, *276*, 10577−10580.

(5) Nakano, S.-i.; Miyoshi, D.; Sugimoto, N. Effects of Molecular Crowding on the Structures, Interactions, and Functions of Nucleic Acids. *Chem. Rev.* **2014**, *114*, 2733−2758.

(6) Cheung, M. S.; Klimov, D.; Thirumalai, D. Molecular Crowding Enhances Native State Stability and Refolding Rates of Globular Proteins. *Proc. Natl. Acad. Sci. U. S. A.* **2005**, *102*, 4753−4758.

(7) Gnutt, D.; Ebbinghaus, S. The Macromolecular Crowding Effect − from in vitro into the Cell. *Biol. Chem.* **2016**, *397*, 37−44.

(8) Zhou, H.-X.; Rivas, G.; Minton, A. P. Macromolecular Crowding and Confinement: Biochemical, Biophysical, and Potential Physiological Consequences. *Annu. Rev. Biophys.* **2008**, *37*, 375−397.

(9) Rivas, G.; Minton, A. P. Macromolecular Crowding In Vitro, In Vivo, and In Between. *Trends Biochem. Sci.* **2016**, *41*, 970−981.

(10) Politou, A.; Temussi, P. A. Revisiting a Dogma: the Effect of Volume Exclusion in Molecular Crowding. *Curr. Opin. Struct. Biol.* **2015**, *30*, 1−6.

(11) Minton, A. P. Models for Excluded Volume Interaction between an Unfolded Protein and Rigid Macromolecular Cosolutes: Macromolecular Crowding and Protein Stability Revisited. *Biophys. J.* **2005**, *88*, 971−985.

(12) Sasahara, K.; McPhie, P.; Minton, A. P. Effect of Dextran on Protein Stability and Conformation Attributed to Macromolecular Crowding. *J. Mol. Biol.* **2003**, *326*, 1227−1237.

(13) Dupuis, N. F.; Holmstrom, E. D.; Nesbitt, D. J. Molecular-Crowding Effects on Single-Molecule RNA Folding/Unfolding Thermodynamics and Kinetics. *Proc. Natl. Acad. Sci. U. S. A.* **2014**, *111*, 8464−8469.

(14) Sung, H.-L.; Sengupta, A.; Nesbitt, D. Smaller Molecules Crowd Better: Crowder Size Dependence Revealed by Single-Molecule FRET Studies and Depletion Force Modeling Analysis. *J. Chem. Phys.* **2021**, *154*, 155101.

(15) Kilburn, D.; Roh, J. H.; Guo, L.; Briber, R. M.; Woodson, S. A. Molecular Crowding Stabilizes Folded RNA Structure by the Excluded Volume Effect. *J. Am. Chem. Soc.* **2010**, *132*, 8690−8696.

(16) Nudler, E.; Mironov, A. S. The Riboswitch Control of Bacterial Metabolism. *Trends Biochem. Sci.* **2004**, *29*, 11−17.

(17) Mironov, A. S.; Gusarov, I.; Rafikov, R.; Lopez, L. E.; Shatalin, K.; Kreneva, R. A.; Perumov, D. A.; Nudler, E. Sensing Small

Molecules by Nascent RNA: A Mechanism to Control Transcription in Bacteria. *Cell* **2002**, *111*, 747−756.
(18) Fiegland, L. R.; Garst, A. D.; Batey, R. T.; Nesbitt, D. J. Single-Molecule Studies of the Lysine Riboswitch Reveal Effector-Dependent Conformational Dynamics of the Aptamer Domain. *Biochemistry* **2012**, *51*, 9223−9233.
(19) Marton Menendez, A.; Nesbitt, D. J. Lysine-Dependent Entropy Effects in the *B. subtilis* Lysine Riboswitch: Insights from Single-Molecule Thermodynamic Studies. *J. Phys. Chem. B* **2022**, *126*, 69−79.
(20) Zimmerman, S. B.; Harrison, B. Macromolecular Crowding Increases Binding of DNA Polymerase to DNA: an Adaptive Effect. *Proc. Natl. Acad. Sci. U. S. A.* **1987**, *84*, 1871−1875.
(21) Ralston, G. B. Effects of "Crowding" in Protein Solutions. *J. Chem. Educ.* **1990**, *67*, 857.
(22) Qu, Y.; Bolen, D. W. Efficacy of Macromolecular Crowding in Forcing Proteins to Fold. *Biophys. Chem.* **2002**, *101-102*, 155−165.
(23) Tokuriki, N.; Kinjo, M.; Negi, S.; Hoshino, M.; Goto, Y.; Urabe, I.; Yomo, T. Protein Folding by the Effects of Macromolecular Crowding. *Protein Sci.* **2004**, *13*, 125−133.
(24) Batra, J.; Xu, K.; Qin, S.; Zhou, H.-X. Effect of Macromolecular Crowding on Protein Binding Stability: Modest Stabilization and Significant Biological Consequences. *Biophys. J.* **2009**, *97*, 906−911.
(25) Sung, H.-L.; Nesbitt, D. J. Effects of Molecular Crowders on Single-Molecule Nucleic Acid Folding: Temperature-Dependent Studies Reveal True Crowding vs Enthalpic Interactions. *J. Phys. Chem. B* **2021**, *125*, 13147−13157.
(26) Sung, H.-L.; Nesbitt, D. J. Single-Molecule FRET Kinetics of the Mn^{2+} Riboswitch: Evidence for Allosteric Mg^{2+} Control of "Induced-Fit" vs "Conformational Selection" Folding Pathways. *J. Phys. Chem. B* **2019**, *123*, 2005−2015.
(27) Fiore, J. L.; Holmstrom, E. D.; Nesbitt, D. J. Entropic Origin of Mg^{2+}-Facilitated RNA Folding. *Proc. Natl. Acad. Sci. U. S. A.* **2012**, *109*, 2902−2907.
(28) Garst, A. D.; Héroux, A.; Rambo, R. P.; Batey, R. T. Crystal Structure of the Lysine Riboswitch Regulatory mRNA Element. *J. Biol. Chem.* **2008**, *283*, 22347−22351.
(29) Sung, H.-L.; Nesbitt, D. J. High Pressure Single-Molecule FRET Studies of the Lysine Riboswitch: Cationic and Osmolytic Effects on Pressure Induced Denaturation. *Phys. Chem. Chem. Phys.* **2020**, *22*, 15853−15866.
(30) Sudarsan, N.; Wickiser, J. K.; Nakamura, S.; Ebert, M. S.; Breaker, R. R. An mRNA Structure in Bacteria That Controls Gene Expression by Binding Lysine. *Genes Dev.* **2003**, *17*, 2688−2697.
(31) Aitken, C. E.; Marshall, R. A.; Puglisi, J. D. An Oxygen Scavenging System for Improvement of Dye Stability in Single-Molecule Fluorescence Experiments. *Biophys. J.* **2008**, *94*, 1826−1835.
(32) Nicholson, D. A.; Sengupta, A.; Nesbitt, D. J. Chirality-Dependent Amino Acid Modulation of RNA Folding. *J. Phys. Chem. B* **2020**, *124*, 11561−11572.
(33) McKinney, S. A.; Joo, C.; Ha, T. Analysis of Single-Molecule FRET Trajectories Using Hidden Markov Modeling. *Biophys. J.* **2006**, *91*, 1941−1951.
(34) Sung, H.-L.; Nesbitt, D. J. Sequential Folding of the Nickel/Cobalt Riboswitch Is Facilitated by a Conformational Intermediate: Insights from Single-Molecule Kinetics and Thermodynamics. *J. Phys. Chem. B* **2020**, *124*, 7348−7360.
(35) Sung, H.-L.; Nesbitt, D. J. Novel Heat-Promoted Folding Dynamics of the *yybP-ykoY* Manganese Riboswitch: Kinetic and Thermodynamic Studies at the Single-Molecule Level. *J. Phys. Chem. B* **2019**, *123*, 5412−5422.
(36) Privalov, P. L. Thermodynamics of Protein Folding. *J. Chem. Thermodyn.* **1997**, *29*, 447−474.
(37) Winzor, D. J.; Jackson, C. M. Interpretation of the Temperature Dependence of Equilibrium and Rate Constants. *J. Mol. Recognit.* **2006**, *19*, 389−407.
(38) Zhou, H.-X. Rate Theories for Biologists. *Q. Rev. Biophys.* **2010**, *43*, 219−293.
(39) Sengupta, A.; Sung, H.-L.; Nesbitt, D. J. Amino Acid Specific Effects on RNA Tertiary Interactions: Single-Molecule Kinetic and Thermodynamic Studies. *J. Phys. Chem. B* **2016**, *120*, 10615−10627.
(40) Szabo, A.; Schulten, K.; Schulten, Z. First Passage Time Approach to Diffusion Controlled Reactions. *Chem. Phys.* **1980**, *72*, 4350−4357.
(41) Pegram, L. M.; Wendorff, T.; Erdmann, R.; Shkel, I.; Bellissimo, D.; Felitsky, D. J.; Record, M. T. Why Hofmeister Effects of Many Salts Favor Protein Folding But Not DNA Helix Formation. *Proc. Natl. Acad. Sci. U. S. A.* **2010**, *107*, 7716−7721.
(42) Courtenay, E. S.; Capp, M. W.; Record, M. T., Jr. Thermodynamics of Interactions of Urea and Guanidinium Salts with Protein Surface: Relationship Between Solute Effects on Protein Processes and Changes in Water-Accessible Surface Area. *Protein Sci.* **2001**, *10*, 2485−2497.
(43) Capp, M. W.; Pegram, L. M.; Saecker, R. M.; Kratz, M.; Riccardi, D.; Wendorff, T.; Cannon, J. G.; Record, M. T. Interactions of the Osmolyte Glycine Betaine with Molecular Surfaces in Water: Thermodynamics, Structural Interpretation, and Prediction of m-Values. *Biochemistry* **2009**, *48*, 10372−10379.
(44) McCluskey, K.; Boudreault, J.; St-Pierre, P.; Perez-Gonzalez, C.; Chauvier, A.; Rizzi, A.; Beauregard, P. B.; Lafontaine, D. A.; Penedo, J. C. Unprecedented Tunability of Riboswitch Structure and Regulatory Function by Sub-Millimolar Variations in Physiological Mg^{2+}. *Nucleic Acids Res.* **2019**, *47*, 6478−6487.
(45) Suddala, K. C.; Wang, J.; Hou, Q.; Walter, N. G. Mg^{2+} Shifts Ligand-Mediated Folding of a Riboswitch from Induced-Fit to Conformational Selection. *J. Am. Chem. Soc.* **2015**, *137*, 14075−14083.
(46) Paudel, B. P.; Rueda, D. Molecular Crowding Accelerates Ribozyme Docking and Catalysis. *J. Am. Chem. Soc.* **2014**, *136*, 16700−16703.
(47) Kilburn, D.; Roh, J. H.; Behrouzi, R.; Briber, R. M.; Woodson, S. A. Crowders Perturb the Entropy of RNA Energy Landscapes to Favor Folding. *J. Am. Chem. Soc.* **2013**, *135*, 10055−10063.
(48) Knowles, D. B.; LaCroix, A. S.; Deines, N. F.; Shkel, I.; Record, M. T. Separation of Preferential Interaction and Excluded Volume Effects on DNA Duplex and Hairpin Stability. *Proc. Natl. Acad. Sci. U. S. A.* **2011**, *108*, 12699−12704.

https://doi.org/10.1021/acs.jpcb.2c03507
J. Phys. Chem. B 2022, 126, 6419−6427